ORIGINAL PAPER

Moonlit swimming: vertical distributions of macrozooplankton and nekton during the polar night

Clare N. Webster · Øystein Varpe ·
Stig Falk-Petersen · Jørgen Berge · Eike Stübner ·
Andrew S. Brierley

Abstract Macrozooplankton (e.g. krill, amphipods and jellyfish) and nekton (e.g. decapod shrimp, squid and fish) are integral parts of pelagic ecosystems, but knowledge of their vertical distributions and migrations during winter at high latitudes is lacking. This study provides the quantification of macrozooplankton and nekton distributions during the polar night in a partially ice-covered high Arctic fjord. In January 2012, mid-water trawls and MIK nets were deployed in Rijpfjorden, Svalbard (80° 18′ N, 22° 15′ E) at three depths (20, 75 and 200 m) day and night.

This article belongs to the special Polar Night issue, coordinated by Ole Jørgen Lønne.

C. N. Webster (✉) · A. S. Brierley
Scottish Oceans Institute, University of St Andrews,
KY16 8LB St. Andrews, UK
e-mail: cnw3@st-andrews.ac.uk

C. N. Webster
Tvärminne Zoological Station, University of Helsinki,
10900 Hanko, Finland

Ø. Varpe · S. Falk-Petersen
Fram Centre, Akvaplan-niva, 9296 Tromsö, Norway

Ø. Varpe · J. Berge · E. Stübner
University Centre in Svalbard, Pb 156, 9171 Longyearbyen,
Norway

Ø. Varpe
Fram Centre, Norwegian Polar Institute, 9296 Tromsö, Norway

S. Falk-Petersen · J. Berge
Faculty of Biosciences, Fisheries and Economics,
University of Tromsö, 9037 Tromsö, Norway

Simultaneously, acoustic volume backscattering strength (a measure of biomass) was recorded using 18-, 38- and 120-kHz echosounders. We observed that the majority of nekton were below the thermocline (>100 m) day and night. A diverse fish community (10 species present) dominated the nekton biomass closely followed by shrimp and squid. Macrozooplankton, mostly large *Calanus* spp. copepods and gelatinous zooplankton, were found throughout the water column, but the majority were above the thermocline day and night. A general additive model with depth, time and moonlight predicted biomass to increase with depth for both macrozooplankton (over the top 100 m) and nekton, but revealed no patterns in biomass over time. The model also indicated that full moon presence increased depth of macrozooplankton backscatter. Our findings suggest a diverse and to some degree active pelagic community during the polar night, and provide some support for the hypothesis that moonlight induces downward vertical migrations of macrozooplankton.

Keywords Arctic · Moon · Zooplankton · Fish · Winter · Pelagic ecology

Introduction

The pelagic is a complex and diverse habitat, with strong vertical structure. Many pelagic ecosystems also have strong seasonality, especially at high latitudes (Varpe 2012). Understanding pelagic ecology therefore requires year-round sampling. Studies of high Arctic pelagic systems in the middle of the polar winter are rare (Melnikov and Kulikov 1980; Weslawski et al. 1991; Fischer and Visbeck 1993; Berge et al. 2009, 2012; Daase et al. 2013) mainly due to the logistical difficulties involved. Basic

knowledge of community composition, biomass and vertical distributions are therefore still lacking at this time of year. In particular, we lack information on the larger organisms that require large nets or trawls to sample them, and very little is known about the behaviour of visually searching predators during the polar night (cf. Kraft et al. 2013). This is a time of year with no daylight and is widely considered to be a time of low or no food intake.

Of the few data we have from the Arctic polar night, recent studies suggest that some high Arctic zooplankton perform diel vertical migration (DVM) during the polar night (Berge et al. 2009, 2012). These are surprising findings as DVM is understood as a day-time avoidance of the surface, driven by the higher efficiency of visually searching predators when light is present (Ohman 1990; Hays 2003). The evidence of polar night DVM is to date built on acoustic information that exposes vertical shifts in acoustic targets, but which has not been able to pinpoint the species or groups of species responsible for the vertical movement. This adds to the need for a better understanding of the pelagic community composition during the polar night. At somewhat lower latitudes, such as Franklin Bay (70°N), Benoit et al. (2010) utilised acoustic techniques to identify DVM of polar cod in mid-January corresponding to twilight times. DVM has also been shown for krill in early February at 70°N in northern Norway (Falk-Petersen and Hopkins 1981).

The main aim of this study was to determine which species of nekton and macrozooplankton are present in the polar night and to investigate where they are in the water column. We also aimed to investigate potential DVM signals. We utilised a combination of two sizes of nets (trawls) with acoustic sampling in an ice-impacted high-latitude environment (Rijpfjorden, Svalbard at 80°N). Due to a lack of sunlight at these high latitudes during the middle of winter (day and night differences indiscernible to the human eye), decreased seasonal food availability at the surface and previous research indicating that zooplankton overwinter at depth there, our two-tiered hypotheses were (1) that macrozooplankton biomass would be highest in the deepest waters and lowest near to the surface and (2) that neither macrozooplankton, micronekton nor nekton would show evidence of DVM. In addition, we took advantage of a full moon event and tested whether moonlight influenced vertical positioning of macrozooplankton and nekton in the water column.

Methods

Sampling took place from the R/V *Helmer Hanssen* during a polar night cruise to Rijpfjorden, Svalbard (80° 18′ N, 22° 15′ E, Fig. 1) on 12 and 13 January 2012. Rijpfjorden is located on the north coast of Nordaustlandet, Svalbard archipelago. The fjord is north-facing and opens widely onto the Arctic Sea via a shelf plateau (100–200 m) that is shallower than the fjord itself. Salinity, temperature and depth distribution were measured using a CTD (Seabird 911 plus) and processed following standard Sea Bird Electronics (SBE) procedures. Times of moon rise and set were calculated using a utility from the United States Naval Observatory, freely available at http://aa.usno.navy.mil/.
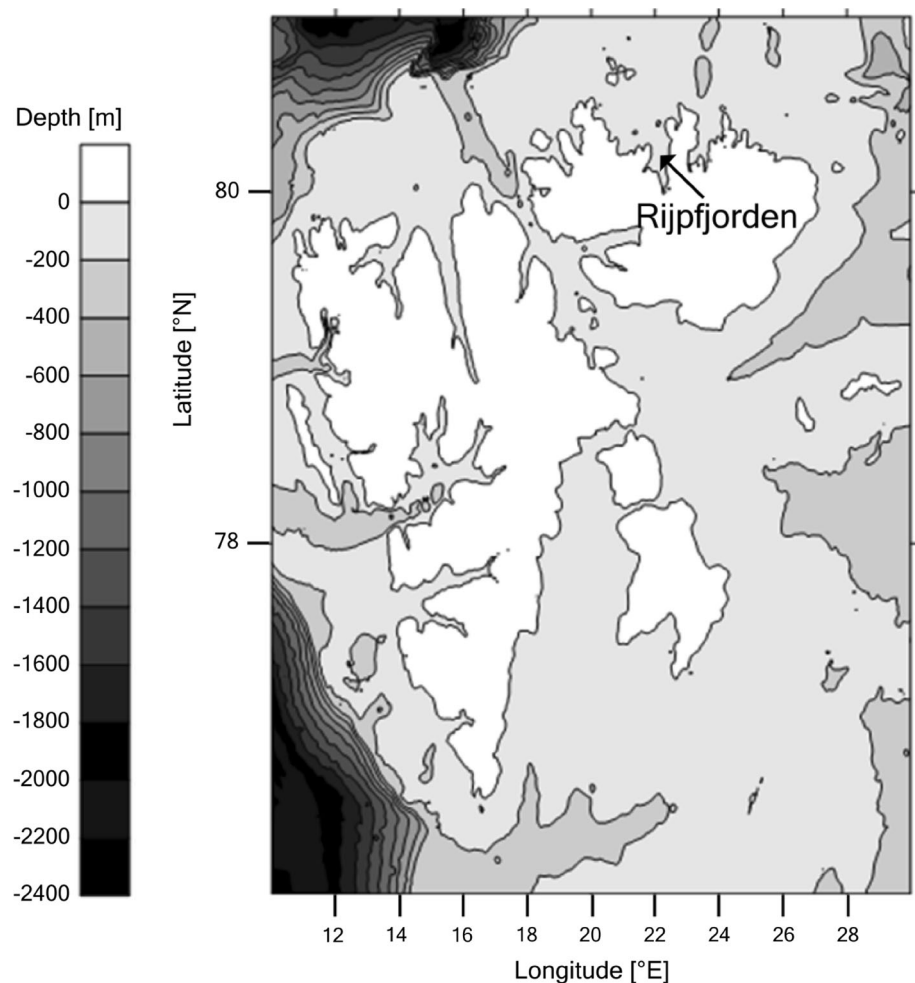
Acoustic sampling

Simrad EK60 echosounders and 18, 38 and 120 kHz transducers are permanently installed on the R/V *Helmer Hanssen* (transducer depth 5.5 m). The system was set to run continuously at maximum ping rate with a pulse duration of 1,024 μs. The three split-beam frequencies (18, 38 and 120 kHz) were calibrated prior to the cruise on the 17 October 2011 using standard calibration techniques (Foote et al. 1987). Post-processing was carried out using the software Echoview v4.9. The nearfield, a range close to the transducer faces within which the transmit pulse is not properly formed, was calculated for 18 kHz at 5 m, 38 kHz at 6.5 m, 120 kHz at 3.5 m and excluded from further processing; for details and explanation see MacLennan and Simmonds (1992). To compensate for signal loss with beam spreading and absorption, time-varied gain (TVG) was applied and amplified noise was removed (Watkins and Brierley 1996). The bottom line identified by the echosounders could not be clearly delineated from fish lying on, or close to, the bottom. Therefore, to avoid biasing fish biomass estimates, all signals from within 10 m of the bottom line were excluded from all analysis.

Acoustic data analyses

To prepare acoustic data for statistical modelling, ping data were resampled by time interval and backscatter (volume backscattering strength or Sv, dB re 1 m^{-1}) and averaged every 5 min/20 cm. The 38-kHz frequency data were used for analyses of nekton distribution, rather than the 18 kHz data, because it has been shown to be optimal for detection of fish species (with swimbladders; sized 5–20 cm) at depths <300 m (Simmonds and MacLennan 2005; Geoffroy et al. 2011) whilst suffering least from 'contamination' from backscatter from macrozooplankton (Madureira et al. 1993; Stanton 1998). For analysis of macrozooplankton backscatter, the highest frequency data (120 kHz) were used. In this study, 'macrozooplankton' refers to animals with a maximum dimension ≥1.3 cm which, by lengths of animals in net catches, includes jellyfish, krill, chaetognaths, hyperiid amphipods and pteropods and excludes copepods. Backscatter that was likely to have originated

from fish targets was removed from 120-kHz data using the difference in mean volume backscattering strength (ΔMVBS) between 120 and 38 kHz (Madureira et al. 1993). Cells with a ΔMVBS of <4 were removed (Geoffroy et al. 2011), leaving only echo energy arising from micronekton and macrozooplankton (Madureira et al. 1993). For 120-kHz data, which were used for analysis of macrozooplankton backscatter, only the top 100 m were available because subtraction of fish echoes left few data with a high signal to noise ratio.

Statistical modelling

To test our hypothesis that DVM did not occur in the polar night, we looked for variation in depth of scattering over a 24-h cycle. To investigate diel movements of either nekton (38 kHz) or micronekton/macrozooplankton (120 kHz), a generalised additive model (GAM) was fit to data from both frequencies. GAMs were used because we did not expect a linear response between backscatter and explanatory variables. GAMs are a regression method that fit smoothing functions between explanatory variables and the response variable and allow for nonlinear relationships (Hastie and Tibshirani 1990). In GAMs, a cross-validated cubic spline smoother (Hamming 1973) replaces the least squares estimate of the multiple linear regression. A Gaussian error distribution was found to be the most appropriate (Swartzman et al. 2002; Zuur et al. 2009), and an identity link function was used to keep predictor variables (e.g. depth) on a linear scale. Specifically, the model validation process was applied on the final GAM (Table 2) by plotting a histogram of residuals and residuals versus fitted values, which revealed normality and homogeneity of variance. Inclusion of an appropriate spatial depth autocorrelation structure into this model was not possible within current computational constraints (Zuur et al. 2009), and interpretive caution is advised when considering the narrow confidence intervals surrounding the depth smoother function. Diagnostic plots to assess independence revealed no temporal autocorrelation. Data were put into two groups (full moon presence and absence) because the difference in residuals indicated that the factor 'Moon' should be included in the model. Akaike information criteria (AIC) were used to assess the candidate GAMs (Akaike 1974) (Table 2).

Table 1 Net deployments in Rijpfjorden from the R/V *Helmer Hanssen* during the multidisciplinary 'Polar Night Cruise' in January 2012

Date	Time (UTC)	Net	Depth (m)
12/01/12	10:25	PT 1	175
	11:46	MIK 1	75
	12:22	MIK 2	225
	21:47	PT 2	225
	22:36	PT 3	200
	23:53	MIK 4	20
13/01/12	00:29	MIK 4	75
	11:04	MIK 5	20
	11:36	MIK 6	75
	12:18	MIK 7	225
	16:04	PT 4	225
	16:44	PT 5	70

MIK MIK net, *PT* pelagic trawl

Statistical modelling and analyses were conducted within the R software environment v2.13.2 using lattice (Sarkar 2008), glme (Hastie and Tibshirani 1990) and mgcv packages (Wood 2006).

Net sampling

To determine species composition, macrozooplankton were sampled with a permanently open MIK ring-net with 1.5-mm mesh size and a diameter of 2 m. Horizontal tows were made on the 12 and 13 January 2012 both at midday and midnight at 2 or 3 depths (Table 1). Tow depth was controlled using the live feed from a Simrad PI depth sensor. After net recovery, the cod end was transferred immediately to a bucket and diluted up to the 9-L mark in the laboratory onboard. Subsamples of 0.6 L were then taken after gentle mixing. The subsamples were fixated on 4 % borax-buffered formaldehyde for later analyses. For nekton and micronekton, five pelagic trawls (mesh size = 1 cm, opening = 9 m) were deployed (Table 1). All animals were identified to the lowest possible taxonomical level and converted to biomass using length or wet weight (see supplementary table). Unless otherwise stated, means are reported with their standard deviation.

Results

The moon was full during the sampling period, and on 12 January, it set at 09:57 UTC and rose at 17:18 UTC. It was up all night and set at 08:32 UTC on the 13 January, not rising until 20:39 UTC. The light of the moon was bright enough that surrounding hills at a range of approx. 3 km
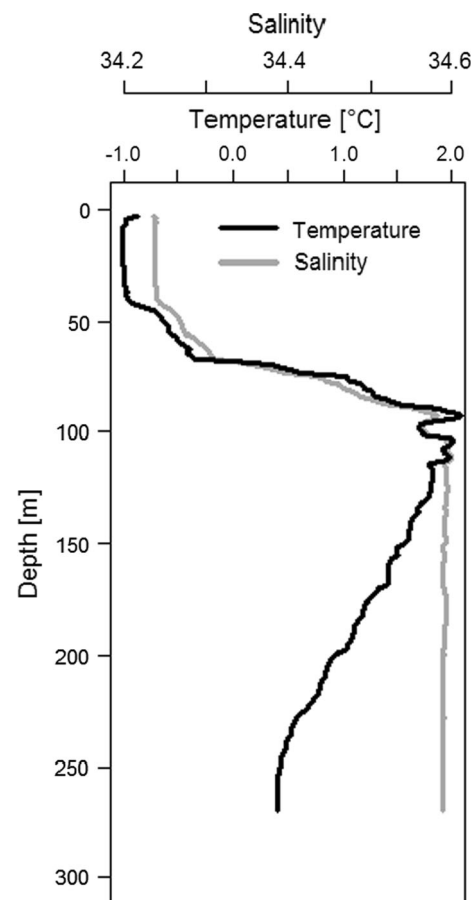

Fig. 2 CTD cast of temperature and salinity on station in Rijpfjorden on 12 January 2012

were visible against the night sky with no visible cloud cover (pers obs). The thermocline was gradual, between 50- and 100-m depth (Fig. 2) with cold temperatures (−1 °C) in the top 50 m. Temperature increased to a maximum of 2 °C at 100 m and then decreased again to 0.5 °C near the bottom which was at a depth of approximately 285 m.

Acoustic backscatter relationships

There was an increase in volume backscatter with depth at all acoustic frequencies (Fig. 3). After subtraction of fish echoes, 120-kHz data (0–100 m) suggest a potential effect of full moon presence, with a decreasing depth of macrozooplankton (Fig. 4), particularly in the top 25 m when the moon is out. Generalised additive models (GAMs) revealed that backscatter had a nonlinear relationship with depth, and an overall increase in backscatter with depth for both frequencies (Fig. 5).

The preferred candidate model (Table 2) explained 81 % of fish backscatter intensity (38 kHz, 0–250 m) and 33 % of micronekton and macrozooplankton backscatter
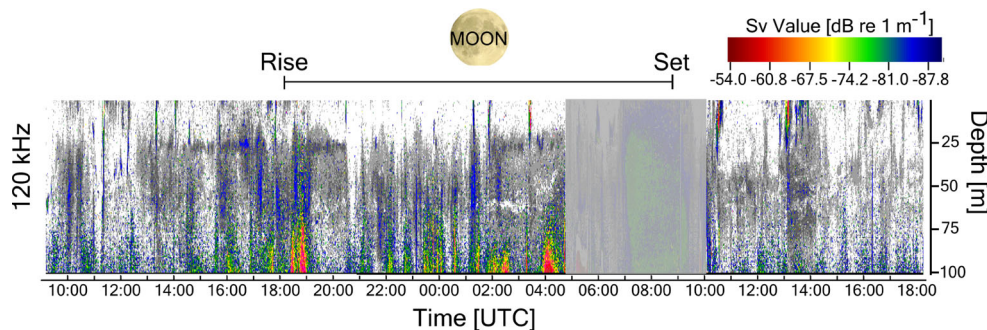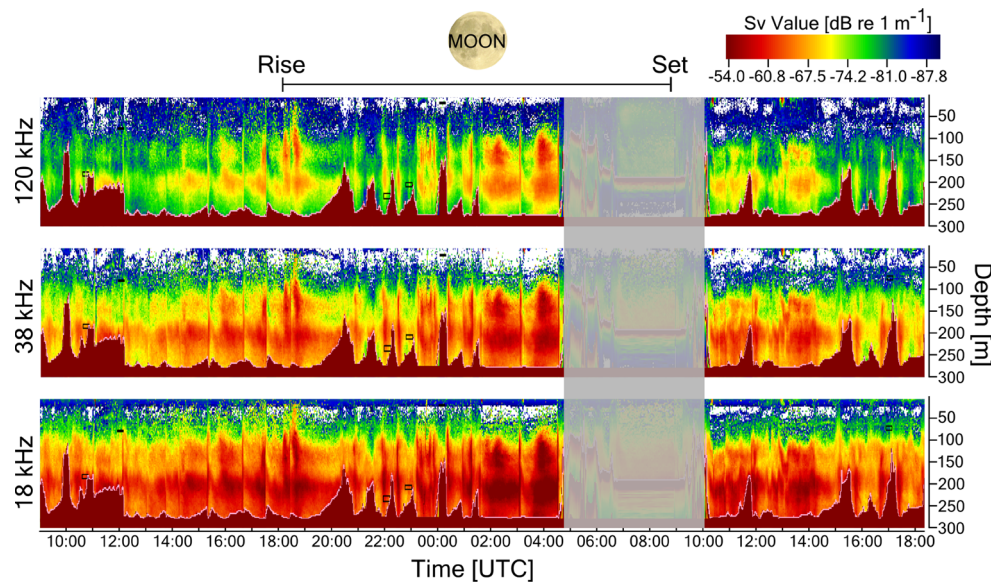
Fig. 4 Acoustic data at 120 kHz after subtraction of fish echoes at sampling station in Rijpfjorden, Svalbard on 12–13 January 2012. Note that only top 100 m are shown (bottom depth approximately 285 m), because high biomass of fish >100 m masked echoes from macrozooplankton. The greyed out area shows when the ship moved away from position temporarily, and these data were not used in analyses

(120 kHz, 0–100 m only). Depth was the best predictor of nekton backscatter intensity explaining 76 % of the variation (Table 2), whereas time alone only explained 3 and 4 % of backscatter deviance for 38 and 120 kHz frequencies, respectively. Moonlight presence/absence interacted with depth to affect macrozooplankton and micronekton backscatter intensity (Table 2). There was a slight decrease in backscatter during full moon in the top 20 m (Fig. 5b). For nekton at full moon, the model predicted a lesser effect (Fig. 5a); however, Sv values indicated (Fig. 6) that depths of strongest scattering grid cells (-50 to -30 dB re 1 m^{-1}) decreased from a minimum of 150 m to a minimum of 100 m during full moon presence.

Net samples

A total of 26 species were collected using the MIK net (Table 3). As the net was open permanently during deployment, it could not be reliably determined whether animals caught were from the target depth or from any depth above it. Biomass of *Calanus* spp. copepods averaged 98.5 ± 51 mg m^{-3} and dominated the macrozooplankton biomass (59 %) at all depths sampled, except two tows: in one at night at 20 m *Beroe cucumis* dominated and, in the other, during the second day at 225 m euphausiids dominated. This was due to relatively low levels of *Calanus* spp. biomass rather than high levels of either *B. cucumis* or euphausiids. Gelatinous zooplankton (including chaetognaths, ctenophores and hydrozoans) made up 26 % of total average biomass, but one must bear in mind that their soft bodies can easily be damaged in plankton nets, leading to probable underestimation of their true biomass. Chaetognaths had an average total biomass of 31.5 ± 16.7 mg m^{-3} and therefore dominated the gelatinous zooplankton biomass overall (72 %). Medusae of three species of gelatinous zooplankton made up the remaining 28 %: the ctenophores *B. cucumis*, *Mertensia ovum* and the hydrozoan *Aglanthe digitale*. The latter dominated the medusae in terms of
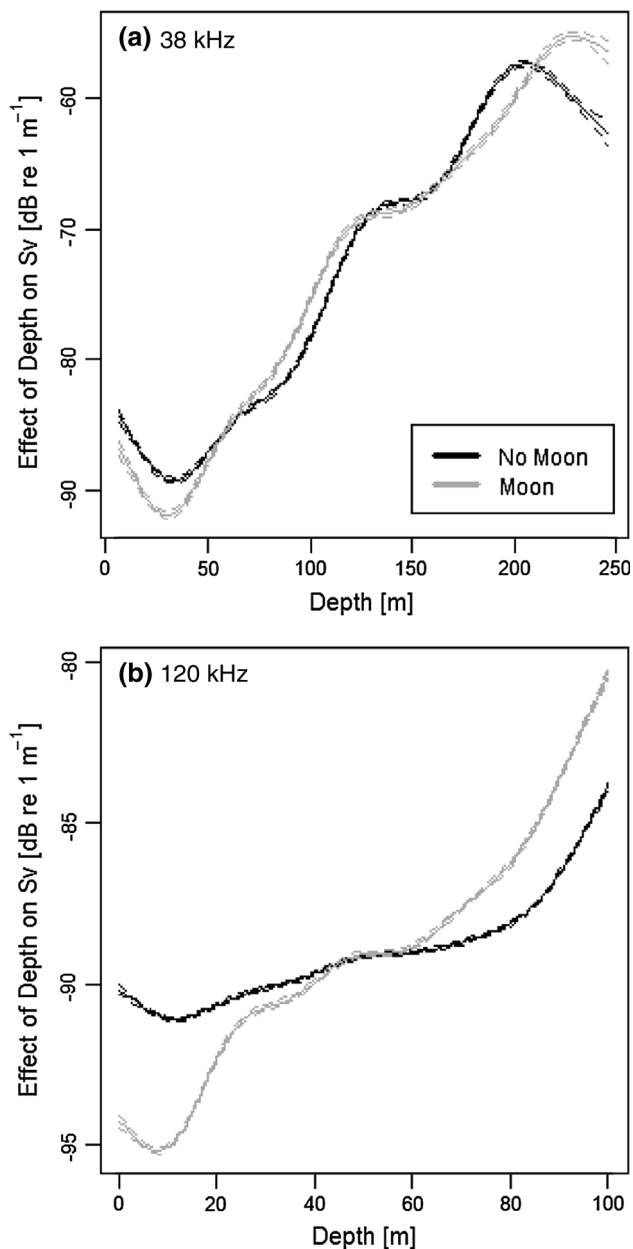
Fig. 5 Smooths of generalised additive model (GAM)-derived effects of depth on **a** 38 kHz (nekton) and **b** 120 kHz (macrozooplankton) data. Note change in scale. Moon presence = *grey*, no moon = *black*. *Dotted lines* are 95 % confidence limits. Please note that inclusion of an appropriate spatial depth autocorrelation structure into this model was not possible within current computational constraints (Zuur et al. 2009), and interpretive caution is advised when considering the narrow confidence intervals surrounding the depth smoother function

numerical abundance at an average of 0.6 ± 0.3 indiv m^{-3} (81 %), but *B. cucumis* dominated the biomass with an average of 10 ± 4.7 mg m^{-3} (83 %), with *A. digitale* at 1.9 ± 1.1 mg m^{-3} (15 %) and *M. ovum* taking up the remaining 2 % with 0.5 ± 0.2 mg m^{-3}. Fragile species such as *M. ovum* are particularly poorly represented due to

the aforementioned sampling artefacts even compared with the more robust *B. cucumis*. A sixth gelatinous zooplankton species, the scyphozoan *Cyanea capillata*, was sampled by pelagic trawl. However, individuals were observed damaged stuck to netting and subsequently frozen so they could not be quantitatively analysed. Pelagic trawls caught 15 species in total (Table 4). On average, over the five trawls, fish represented 41 ± 15 % of the nekton biomass, decapod shrimp (*Pandalus borealis*) 37 ± 11 % and squid (*Gonatus fabricii*) 19 ± 9.6 %. Polar cod (*Boreogadus saida*) and Atlantic cod (*Gadus morhua*) contributed 85 ± 5 and 13 ± 5 % of the fish biomass, respectively, with other fish species contributing 1 ± 2 % of the fish biomass. A broad overview by biomass of taxonomic grouping from both net types (Fig. 7) supports the large biomass of nekton at depth observed with the 38-kHz echosounder. Very few fish (5.7 × 10^{-4} indiv m^{-3}) and no squid or shrimp were found in the pelagic trawl taken at 70-m depth.

Discussion

Nekton

Nekton backscattering intensity had a strong positive relationship with depth, being found mostly below the thermocline in warmer waters. This is not unexpected as a study of polar cod (*Boreogadus saida*) in Amundsen Bay (71°N) also reported large, localised aggregations of *B. saida* in deep, warmer waters during winter (Geoffroy et al. 2011). They suggest aggregation distributions are driven by spawning, prey distribution, temperature and a predator avoidance adaptation including avoidance of ringed seals (*Phoca hispida*) (Benoit et al. 2008; Geoffroy et al. 2011). *B. saida* was the dominant fish species present here, and aggregation features visible in echograms from this study (Fig. 3) are similar to aggregations in the echograms of Geoffroy et al. (2011). With the thermocline above 100 m (approx. 50–100 m), these data suggest nekton migrants probably did not cross it, again similar to the findings in the Canadian Arctic (Benoit et al. 2010; Geoffroy et al. 2011). Above the thermocline, the temperature drops to sub-zero, which can slow fish movement and freeze blood of species such as Atlantic cod (*Gadus morhua*) and haddock (*Melanogrammus aeglefinus*) (Castonguay and Cyr 1998). *B. saida* synthesises anti-freeze proteins and lives in sub-zero temperatures, but it has been suggested that its vertical movements through the thermocline are limited (Melnikov and Chernova 2013).

Mean biomass of fish species (56 mg m^{-3}) was similar to mean biomass of decapod shrimp (*Pandalus borealis*, 42 mg m^{-3}), which are also important predators of macrozooplankton such as euphausiids, amphipods and

Table 2 Generalised additive model (GAM) selection process including depth, time and moon presence/absence as explanatory variables for backscatter (Sv)

Model number	Model structure	Nekton (38 kHz)			Macrozooplankton (120 kHz)		
		r^2_{adj}	ΔAIC	AIC	r^2_{adj}	ΔAIC	AIC
1	Sv ~ s(Depth)	0.76	0	44,075	0.23	0	30,867
2	Sv ~ s(Time)	0.03	+519,887	555,710	0.04	+37,034	67,901
3	Sv ~ s(Depth) + s(Time)	0.77	−19,014	25,061	0.27	−9,521	21,346
4	Sv ~ s(Depth) + f(Moon)	0.77	−23,649	20,426	0.25	−14,683	16,184
5	Sv ~ s(Depth) + s(Time) + f(Moon)	0.78	−37,988	6,087	0.29	−18,290	12,577
6	Sv ~ s(Depth) × (fMoon) + s(Time)[a]	0.81	−41,970	**2,105**	0.33	−28,971	**1,896**

Models were selected using Akaike information criteria (AIC). Model 6 was selected as the preferred model for both the 38- and 120-kHz data (full equation given as footnote). ΔAIC indicates the step-wise reduction (or increase) in AIC as variables are added to or removed from the first model—final AICs are given in bold text

[a] $Sv_{is} = \alpha + f(Depth_s) * factor(Moon) + f(Time_i) + \varepsilon_{is}$ $\varepsilon_{is} \sim N(0, \sigma^2)$ where Sv_{is} is Sv values at time i at depth s, α is the intercept, f is the smoothing function, and ε_{is} are residuals independently, normally distributed with expectation 0 and variance σ^2
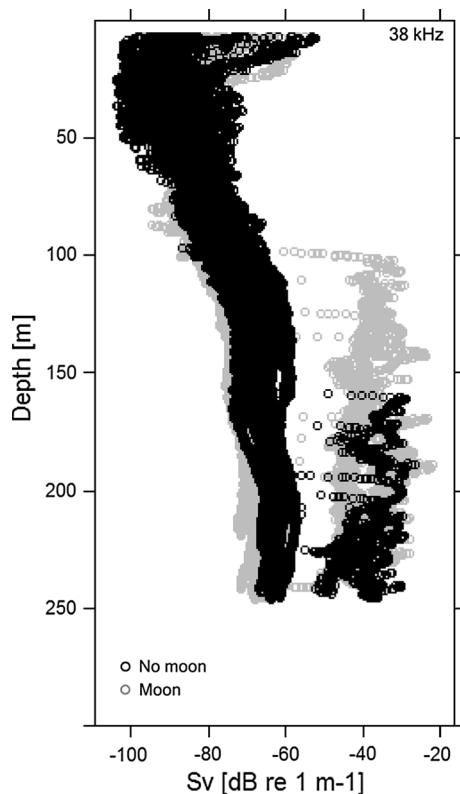

Fig. 6 Plot of 38 kHz volume backscattering strength or Sv, dB re 1 m^{-1} against depth. Moon presence = *grey*, no moon = *black*. Points represent Sv averaged every 5 min/20 cm. There is some evidence of a group of stronger scatterers (−50 to −30 dB re 1 m^{-1}) with a partially decreased depth distribution during the full moon. The response to moon presence is weak, especially compared with the response of macrozooplankton

chaetognaths (Savenkoff et al. 2006), as are squid (*Gonatus fabricii*) (Nesis 1965; Kristensen 1984). *P. borealis* and *G. fabricii* have long antennae and tentacles, respectively,

which may contribute to a decreased reliance on vision for prey capture. The high backscatter values of the group of nekton that appear to partially decrease their depth distribution during moon presence could be an indication of dense fish shoals or larger fish individuals rather than aggregations of *P. borealis* or *G. fabricii* (Swartzman et al. 2002). Studies from other regions have linked dive depth of predators of nekton (birds, mammals, swordfish and sharks) to lunar cycles (Wilson et al. 1993; Horning and Trillmich 1999; Schaefer and Fuller 2002; Abascal et al. 2010; Saunders et al. 2011; Libini and Khan 2012), but there are key local differences due to size of prey and oceanographic features (Benoit-Bird et al. 2009; Saunders et al. 2011). There are, however, presently no such studies from the high north during the polar night.

Macrozooplankton

The model (applied to top 100 m only) predicted a descent of macrozooplankton during full moon. Observed directly from processed echosounder data, mean Sv decreased during full moon in the top 20 m. Moonlight can be detected by mesozooplankton (copepods) to around 100–140 m depth (Båtnes et al. this issue) so it is possible that moonlight at least partially explains the response of macrozooplankton at these depths. Over sixty years ago, Moore (1950) observed that during the full moon, diel migrants were not found <100 m and Patten (1971) showed that moonlight increased fish predation on salmon larvae. Gliwicz (1986) first showed that moonlight can influence DVM of freshwater zooplankton due to higher death rates of the zooplankton during new moon, as planktivorous fish avoided increased predation during the full moon. During a study of vertical migration by krill (*Meganyctiphanes norvegica*) in the

Table 3 Species presence indicated by a black dot for each MIK net taken during 12 and 13 January 2012 in Rijpfjorden, Svalbard

Species	Day 75 m	Day 225 m	Night 20 m	Night 75 m	Day 20 m	Day 75 m	Day 225 m
Beroe cucumis	•	•	•	•	•	•	•
Mertensia ovum		•	•	•			
Aglanthe digitale	•	•	•	•	•	•	•
Thysanoessa inermis	•	•	•	•	•	•	•
T. longicaudata	•	•	•	•	•	•	
T. raschii		•	•		•	•	•
Eukrohnia hamata ≥20 mm	•	•	•	•	•	•	•
E. hamata ≥10 mm	•	•	•	•	•	•	•
Sagitta elegans ≥20 mm	•	•	•	•	•	•	•
S. elegans ≥10 mm	•	•	•	•	•	•	•
Hyperia galba				•			
Hyperoche medusaraum		•		•		•	•
Themisto abyssorum ≥5 mm	•		•	•	•	•	•
T. libellula ≥5 mm	•			•	•		
Apherusa glacialis	•	•	•	•	•	•	•
Erythrops erythropthalma		•					
Clione limacina ≥5 mm	•	•		•	•	•	•
Limacina helicina ≥5 mm		•	•			•	•
Calanus finmarchicus AM	•	•		•	•	•	•
C. finmarchicus AF	•	•		•	•	•	•
C. finmarchicus CV	•	•		•	•	•	•
C. finmarchicus CIV	•	•		•	•	•	•
C. glacialis AM	•	•	•	•	•	•	•
C. glacialis AF	•	•	•	•	•	•	•
C. glacialis CV	•	•	•	•	•	•	•
C. glacialis CIV	•	•	•	•	•	•	•
C. hyperboreus AM	•	•	•		•	•	•
C. hyperboreus AF	•	•		•	•	•	•
C. hyperboreus CV	•	•		•	•	•	•
C. hyperboreus CIV	•			•	•	•	
Metridia longa AM	•	•	•	•	•	•	•
M. longa AF	•	•	•	•	•	•	•
M. longa CV	•	•	•	•	•	•	•
Paraeuchaeta norvegica AM						•	•
P. norvegica AF	•	•		•	•	•	•
P. norvegica CV	•				•		
Bradyidius similis		•				•	•
Polychaete larvae		•					
Gaetanus tenuispinus		•					
Appendicularia larvae			•				
Caligus spp.			•				

M male, *F* female, *CV, CIV, CIII* copepodite stages

Ligurian Sea using a 153-kHz Acoustic Doppler Current Profiler (ADCP), Tarling et al. (1999) made two important observations: (1) as moonrise moved progressively further away from sunset so did the sinking of *M. norvegica* (*i.e.* they sank when the moon rose) and (2) during a lunar eclipse, *M. norvegica* remained at the surface. Similarly, Pinot and Jansá (2001) utilised a 153-kHz ADCP in the Mediterranean Sea and reported

Table 4 Species presence indicated by a black dot for each pelagic trawl net taken during 12 and 13 January 2012 in Rijpfjorden, Svalbard

Species	Day 175 m	Night 225 m	Night 200 m	Day 225 m	Day 70 m
Todarodes sagittatus	●	●	●	●	
Pandalus borealis	●	●	●	●	
Euphausiids	●	●	●	●	●
Boreogadus saida	●	●	●	●	●
Gadus morhua	●	●	●	●	●
Melanogrammus aeglefinus	●	●	●	●	
Reinhardtius hippoglossoides	●	●	●	●	●
Mallotus villosus	●				
Sebastes spp.	●	●	●	●	●
Leptoclinus maculatus	●				
Liparis spp.					
Cyanea capillata	●	●	●	●	●

that zooplankton preferred deeper layers during the full moon. Our short-term observations and model predictions of increased depth of macrozooplankton during a full moon support the conclusions of Tarling et al. (1999), which state that moonlight is the exogenous cue that sets an endogenous lunar rhythm (Benoit-Bird et al. 2009). On the other hand, some studies make no mention of lunar influence, possibly because either they have not tested this hypothesis with their data (Cisewski et al. 2010) or that other factors have a primary influence in different areas. In addition, bioluminescent light is visible during the polar night and it is possible that this light source plays a role in determining vertical movements in animals that we could not account for (Haddock et al. 2010; Berge et al. 2012).

Macrozooplankton net counts were not robust enough for statistical analysis due to the permanently open operation of the nets and sampling difficulties affecting estimates of gelatinous zooplankton biomass. However, in terms of macrozooplankton biomass, gelatinous zooplankton still made up almost a third of all macrozooplankton sampled. This is likely a substantial underestimation but is still an indication of their relative importance for the mid-winter Arctic pelagic ecosystem. Due to sampling constraints, there are few data available for comparison, but abundances of *Aglanthe digitale* were approximately two orders of magnitude less than summer time abundances at 20 m in the Canada basin, whilst abundances of *Beroe cucumis* were up to four times greater (Raskoff et al. 2005; Purcell et al. 2010; Lilley et al. 2011). The dominance of *Calanus* spp. copepods is consistent with previous studies in this region and in the wider Arctic Sea (Falk-Petersen et al. 2009). Surprisingly, Adult *Metridia longa* and *Calanus* spp. copepods were found at all depths with higher biomasses at 20 and 75 m than at 225 m (see also Daase et al. 2013). Previous research has indicated that they would typically be overwintering at depth
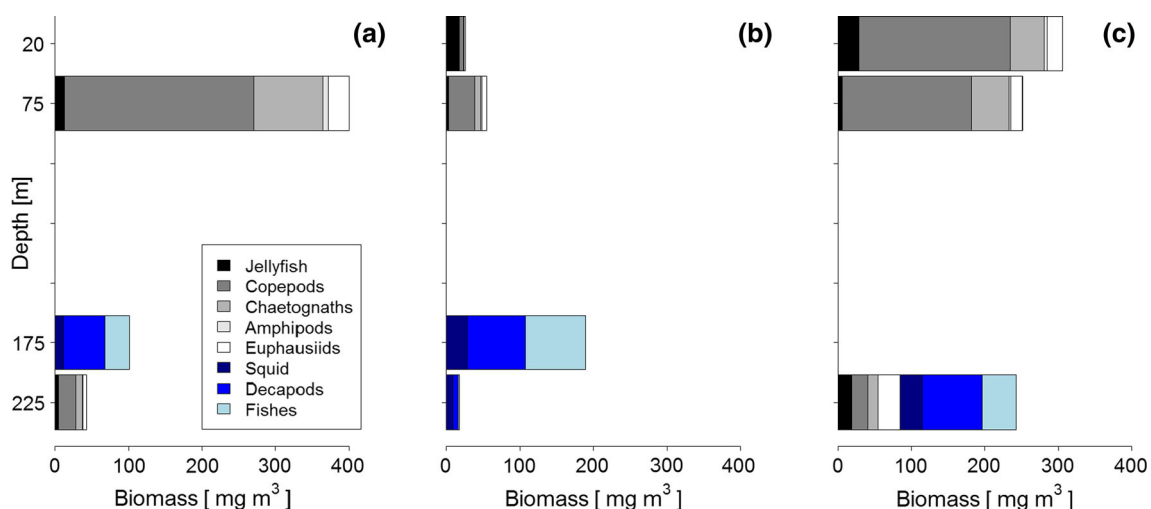

Fig. 7 Biomass (dry weight in mg m^{-3}) of MIK net data in greyscale and pelagic trawl data in blue, **a** 12 January daytime sampling, **b** 12–13 January midnight (time of full moon), **c** 13 January daytime sampling. (Color figure online)

(Hays 1995; Hirche and Kosobokova 2011) and it is possible that this unexpected vertical distribution of copepods near the surface is due to high densities of nekton predators at depth.

References

Abascal FJ, Mejuto J, Quintans M, Ramos-Cartelle A (2010) Horizontal and vertical movements of swordfish in the Southeast Pacific. ICES J Mar Sci 67:466–474

Akaike H (1974) New look at statistical-model identification. IEEE Trans Autom Contr 19:716–723

Benoit D, Simard Y, Fortier L (2008) Hydroacoustic detection of large winter aggregations of Arctic cod (*Boreogadus saida*) at depth in ice-covered Franklin Bay (Beaufort Sea). J Geophys Res Oceans 113:1–9

Benoit D, Simard Y, Gagne J, Geoffroy M, Fortier L (2010) From polar night to midnight sun: photoperiod, seal predation, and the diel vertical migrations of polar cod (*Boreogadus saida*) under landfast ice in the Arctic Ocean. Polar Biol 33:1505–1520

Benoit-Bird KJ, Au WWL, Wisdom DW (2009) Nocturnal light and lunar cycle effects on diel migration of micronekton. Limnol Oceanogr 54:1789–1800

Berge J, Cottier F, Last KS, Varpe O, Leu E, Soreide J, Eiane K, Falk-Petersen S, Willis K, Nygard H, Vogedes D, Griffiths C, Johnsen G, Lorentzen D, Brierley AS (2009) Diel vertical migration of Arctic zooplankton during the polar night. Biol Lett 5:69–72

Berge J, Batnes AS, Johnsen G, Blackwell SM, Moline MA (2012) Bioluminescence in the high Arctic during the polar night. Mar Biol 159:231–237

Castonguay M, Cyr DG (1998) Effects of temperature on spontaneous and thyroxine-stimulated locomotor activity of Atlantic cod. J Fish Biol 53(2):303–313

Cisewski B, Strass VH, Rhein M, Kraegefsky S (2010) Seasonal variation of diel vertical migration of zooplankton from ADCP backscatter time series data in the Lazarev Sea, Antarctica. Deep-Sea Res Part I Oceanogr Res Pap 57:78–94

Daase M, Varpe Ø, Falk-Petersen S (2013) Non-consumptive mortality in copepods: occurrence of *Calanus* spp. carcasses in the Arctic Ocean during winter. J Plankton Res. doi:10.1093/plankt/fbt079

Falk-Petersen S, Hopkins CCE (1981) Zooplankton sound scattering layers in North Norwegian fjords: interactions between fish and krill shoals in a winter situation in Ullsfjorden and Øksfjorden. Kieler Meeresforsch Sonderh 5:191–201

Falk-Petersen S, Mayzaud P, Kattner G, Sargent JR (2009) Lipids and life strategy of Arctic *Calanus*. Mar Biol Res 5:18–39

Fischer J, Visbeck M (1993) Seasonal variation of the daily zooplankton migration in the Greenland Sea. Deep Sea Res Part I Oceanogr Res Pap 40:1547–1557

Foote KG, Knudsen HP, Vestnes G, MacLennan DN, Simmonds EJ (1987) Calibration of acoustic instruments for fish density estimation: a practical guide. ICES Coop Res Rep 144:1–81

Geoffroy M, Robert D, Darnis G, Fortier L (2011) The aggregation of polar cod (*Boreogadus saida*) in the deep Atlantic layer of ice-covered Amundsen Gulf (Beaufort Sea) in winter. Polar Biol 34:1959–1971

Gliwicz ZM (1986) A lunar cycle in zooplankton. Ecology 67:883–897

Haddock SHD, Moline M, Case JF (2010) Bioluminescence in the Sea. Annu Rev Mar Sci 2:443–493

Hamming RW (1973) Numerical methods for scientists and engineers. McGraw-Hill, New York

Hastie T, Tibshirani R (1990) Exploring the nature of covariate effects in the proportional hazards model. Biometrics 46:1005–1016

Hays GC (1995) Ontogenetic and seasonal variation in the diel vertical migration of the copepods *Metridia lucens* and *Metridia longa*. Limnol Oceanogr 40:1461–1465

Hays GC (2003) A review of the adaptive significance and ecosystem consequences of zooplankton diel vertical migrations. Hydrobiologia 503:163–170

Hirche HJ, Kosobokova KN (2011) Winter studies on zooplankton in Arctic seas: the Storfjord (Svalbard) and adjacent ice-covered Barents Sea. Mar Biol 158:2359–2376

Horning M, Trillmich F (1999) Lunar cycles in diel prey migrations exert a stronger effect on the diving of juveniles than adult Galapagos fur seals. Proc R Soc B 266:1127–1132

Kraft A, Berge J, Varpe Ø, Falk-Petersen S (2013) Feeding in Arctic darkness: mid-winter diet of the pelagic amphipods *Themisto abyssorum* and *T. libellula*. Mar Biol 160:241–248

Kristensen TK (1984) Biology of the squid *Gonatus fabricii* from West Greenland waters. Medd Groen Biosci 13:3–17

Libini CL, Khan SA (2012) Influence of lunar phases on fish landings by gillnetters and trawlers. Indian J Fish 59:81–87

Lilley MKS, Beggs SE, Doyle TK, Hobson VJ, Stromberg KHP, Hays GC (2011) Global patterns of epipelagic gelatinous zooplankton biomass. Mar Biol 158:2429–2436

MacLennan DN, Simmonds EJ (1992) Fisheries acoustics. Chapman and Hall, London

Madureira LSP, Everson I, Murphy EJ (1993) Interpretation of acoustic data at two frequencies to discriminate between Antarctic krill (*Euphausia superba dana*) and other scatterers. J Plankton Res 15:787–802

Melnikov IA, Chernova NV (2013) Characteristics of under-ice swarming of polar cod *Boreogadus saida* (Gadidae) in the Central Arctic Ocean. J Icthyol 53:7–15

Melnikov IA, Kulikov AS (1980) Cryopelagic fauna of the Central Arctic Basin. In: Vinogradov ME, Melnikov IA (eds) Biology of the Central Arctic Basin. Nauka, Moscow, pp 97–111

Moore HB (1950) The relation between the scattering layer and the Euphausiacea. Biol Bull 99:181–212

Nesis KN (1965) Distribution and feeding of young squids *Gonatus fabricii* in the Labrador Sea and the Norwegian Sea. Oceanology 5:102–108

Ohman MD (1990) The demographic benefits of diel vertical migration by zooplankton. Ecol Monogr 60:257–281

Patten BG (1971) Increased predation by torrent sculpin, *Cottus rhotheus*, on coho salmon fry, *Oncorhynchus kisutch*, during moonlight nights. Can J Fish Aquat Sci 28:1352

Pinot JM, Jansá J (2001) Time variability of acoustic backscatter from zooplankton in the Ibiza Channel (western Mediterranean). Deep Sea Res Part I Oceanogr Res Pap 48:1651–1670

Purcell JE, Hopcroft RR, Kosobokova KN, Whitledge TE (2010) Distribution, abundance, and predation effects of epipelagic

ctenophores and jellyfish in the western Arctic Ocean. Deep Sea Res Part I Oceanogr Res Pap 57:127–135

Raskoff KA, Purcell JE, Hopcroft RR (2005) Gelatinous zooplankton of the Arctic Ocean: in situ observations under the ice. Polar Biol 28:207–217

Sarkar D (2008) Lattice: multivariate data visualization with R. Springer, New York

Saunders RA, Royer F, Clarke MW (2011) Winter migration and diving behaviour of porbeagle shark, *Lamna nasus*, in the Northeast Atlantic. ICES J Mar Sci 68:166–174

Savenkoff CL, Savard BM, Chabot D (2006) Main prey and predators of northern shrimp (*Pandalus borealis*) in the northern Gulf of St. Lawrence during the mid-1980s, mid-1990s, and early 2000s. Can Tech Rep Fish Aquat Sci 2639:28

Schaefer KM, Fuller DW (2002) Movements, behaviour, and habitat selection of bigeye tuna (*Thunnus obesus*) in the eastern equatorial Pacific, ascertained through archival tags. Fish Bull 100:765–788

Simmonds EJ, MacLennan DN (2005) Fisheries acoustics: theory and practice. Blackwell Science, London

Swartzman G, Napp J, Brodeur R, Winter A, Ciannelli L (2002) Spatial patterns of pollock and zooplankton distribution in the Pribilof Islands, Alaska nursery area and their relationship to pollock recruitment. ICES J Mar Sci 59:1167–1186

Tarling GA, Buchholz F, Matthews JBL (1999) The effect of a lunar eclipse on the vertical migration behaviour of *Meganyctiphanes norvegica* (Crustacea : Euphausiacea) in the Ligurian Sea. J Plankton Res 21:1475–1488

Varpe O (2012) Fitness and phenology: annual routines and zooplankton adaptations to seasonal cycles. J Plankton Res 34:267–276

Watkins JL, Brierley AS (1996) A post-processing technique to remove background noise from echo integration data. ICES J Mar Sci 53:339–344

Weslawski JM, Kwasniewski S, Wiktor J (1991) Winter in a Svalbard fjord ecosystem. Arctic 44:115–123

Wilson RP, Puetz K, Bost CA, Culik BM, Bannasch R, Reins T, Adelung D (1993) Diel dive depth in penguins in relation to diel vertical migration of prey—whose dinner by candlelight. Mar Ecol Prog Ser 94:101–104

Wood SN (2006) Generalized additive models: an introduction. Chapman and Hall, London

Zuur AF, Ieno EN, Walker NJ, Saveliev AA, Smith GM (2009) Mixed effects models and extensions in ecology. Springer, Berlin